Frequency Domain System Identification for a Small, Low-Cost, Fixed-Wing UAV

Andrei Dorobantu*, Austin M. Murch†, Bernie Mettler‡, and Gary J. Balas§,
Department of Aerospace Engineering & Mechanics
University of Minnesota, Minneapolis, MN, 55455, USA

This paper describes a practical and systematic procedure for modeling and identifying the flight dynamics of small, low-cost, fixed-wing uninhabited aerial vehicles (UAVs). The procedure is applied to the Ultra Stick 25e flight test vehicle of the University of Minnesota UAV flight control research group. The procedure hinges on a general model structure for fixed-wing UAV flight dynamics derived using first principles analysis. Wind tunnel tests and simplifying assumptions are applied to populate the model structure with an approximation of the Ultra Stick 25e flight dynamics. This baseline model is used to design informative flight experiments for the subsequent frequency domain system identification. The final identified model is validated against separately acquired time domain flight data.

Nomenclature

m	Mass, kg
I_x, I_y, I_z	Moments of inertia, $kg\ m^2$
V	Airspeed, m/s
α	Angle-of-attack, rad
β	Angle of sideslip, rad
X, Y, Z	Positions, m
u, v, w	Body axis velocities, m/s
ϕ, θ, ψ	Attitude angles, rad
p, q, r	Body axis angular rates, rad/s
δ_{elev}	Elevator deflection, rad
δ_{ail}	Aileron deflection, rad
δ_{rud}	Rudder deflection, rad
S	Spectral density function
γ^2	Coherence function

I. Introduction

Uninhabited Aerial Vehicles (UAVs) have become popular as flight test platforms in the domain of flight control research. The vehicles are attractive due to their compact dimensions, low cost, and limited risk of damage or harm in the event of failure. An important task for the development of UAV flight test platforms is modeling and identifying the aircraft dynamics. Accurate models of UAV flight dynamics are generally unavailable due to the custom design of the airframes. However, such models are required to characterize aircraft behavior and determine stability and performance properties. The primary objective of the work presented in this paper is to develop a practical and systematic procedure for modeling and identifying the flight dynamics of small, low-cost, fixed-wing UAVs.

*Graduate Student, AIAA Student Member
†Senior Research Associate, AIAA Senior Member
‡Assistant Professor, AIAA Member
§Professor, AIAA Associate Fellow

System identification provides a way to determine aircraft flight dynamics based on data obtained through flight experiments. In combination with first principle methods, it allows the determination of complete and accurate models. Various identification techniques have been developed to model small-scale aircraft dynamics. Reference 1 provides a background on system identification theory. Reference 2 is a comprehensive summary on general aircraft modeling and the practical application of system identification. In addition, a vast quantity of papers on modeling and novel identification techniques for small fixed-wing and rotary-wing UAVs have been published in recent literature.[3–5]

This paper describes a practical and systematic procedure for modeling and system identification and applies it to determine the flight dynamics of the Ultra Stick 25e. This aircraft is commercially available and serves as the primary flight test vehicle for the University of Minnesota UAV flight control research group.[6] The Ultra Stick 25e is a small, low-cost, fixed-wing, radio controlled aircraft. It is equipped with standard elevator, aileron, and rudder control surfaces. The aircraft is powered by an electric motor that drives a propeller. The aircraft is shown in Figure 1.

Figure 1. Ultra Stick 25e flight test vehicle.

The system identification techniques described in this paper are based on frequency domain methods to obtain a physically meaningful parametric model of the aircraft dynamics. This approach has been previously applied to small-scale rotorcraft UAVs.[4] Frequency domain identification has several advantages, the most general one being that it is founded in linear systems theory. Therefore, it lends itself to linear control design and analysis. Additionally, the user has direct control over the frequency ranges to be modeled, and the ability to exploit any known structures in the dynamics. Uncertainty and disturbance models can easily be created, which are useful for robust control.

The main contribution of the work summarized in this paper is a systematic procedure for modeling and identifying the flight dynamics of small, low-cost, fixed-wing UAVs. The procedure is rigorous due to its foundation in physics-based modeling and linear systems theory. At the core of the procedure is a general model structure for fixed-wing UAV flight dynamics that is is derived from first principles rigid-body kinematic and aerodynamic theory. Wind tunnel tests and simplifying assumptions are used to determine aerodynamic derivatives, giving a first approximation of the aircraft dynamics. This baseline model is used to design informative flight tests needed to collect data to generate experimental frequency responses. The frequency responses are then used to estimate the parameters of the model. Finally, the identified model is validated against separately acquired time history flight data. In this work, the CIFER software package is used for the entire analysis and data processing involved in the identification process.[7]

Remaining sections of this paper are organized as follows: a general fixed-wing aircraft flight dynamics model structure is derived from first principles in Section II. Properties of the Ultra Stick 25e and the preliminary analysis required to obtain a baseline model of the flight dynamics are described in Section III. Section IV details the design of flight experiments and a brief overview of the theoretical background to frequency domain system identification. The identification results are presented. Finally, the identified model is validated with time domain data in Section V. Concluding remarks are given in Section VI.

II. Fixed-Wing Aircraft Flight Dynamics

The equations of motion for conventional fixed-wing aircraft can be derived analytically from the Newton-Euler equations, where the main task is to determine expressions for the external forces. These forces include gravitational forces, propulsion forces, and aerodynamic forces. The resulting equations of motion are nonlinear and coupled. A linear model is derived by assuming small perturbations from equilibrium, and serves as the basis for system identification in this paper. The nonlinear equations of motion are linearized

about a particular equilibrium flight condition, or operating point. An operating point is defined by airspeed, altitude, climb rate, and turn rate. Flight experiments are conducted at a given operating point, and the model is identified and validated accordingly. To simplify the dynamics, the longitudinal dynamics are assumed to be decoupled from the lateral/directional dynamics. Further, throttle is assumed to be constant.

The simplest form of the equations of motion is taken in the body axis reference frame of the aircraft and assumes a flat Earth coordinate system. Twelve states are required to describe the aircraft rigid-body dynamics: three inertial positions $[X, Y, Z]$, three body-axis velocities $[u, v, w]$, three attitude angles $[\phi, \theta, \psi]$, and three body-axis angular rates $[p, q, r]$. Detailed derivations of the aircraft equations of motion are available in flight dynamics textbooks, such as References 2 and 8. This paper provides a brief overview of conventional fixed-wing aircraft dynamics and the assumptions required to simplify the model.

1. Longitudinal Dynamics

The longitudinal flight dynamics of fixed-wing aircraft are described by the set of states $x = [u, w, q, \theta]^T$, which include body x-axis velocity u [m/s], body z-axis velocity w [m/s], pitch rate q [rad/s], and pitch angle θ [rad]. The primary control surface input in this longitudinal dynamics model is the elevator deflection δ_{elev} [rad]. The linearized longitudinal equations of motion are given by the system in Equation 1.

$$M_{lon}\dot{x} = A'_{lon}x + B'_{lon}\delta_{elev} \tag{1}$$

where

$$M_{lon} = \begin{bmatrix} m & 0 & 0 & 0 \\ 0 & m & 0 & 0 \\ 0 & 0 & I_y & 0 \\ 0 & 0 & 0 & 1 \end{bmatrix} \quad A'_{lon} = \begin{bmatrix} X_u & X_w & X_q - mW_e & -mgcos\theta_e \\ Z_u & Z_w & Z_q + mU_e & -mgsin\theta_e \\ M_u & M_w & M_q & 0 \\ 0 & 0 & 1 & 0 \end{bmatrix} \quad B'_{lon} = \begin{bmatrix} X_{\delta_{elev}} \\ Z_{\delta_{elev}} \\ M_{\delta_{elev}} \\ 0 \end{bmatrix}$$

The mass matrix M_{lon} represents the inertial properties of the airframe pertaining to the longitudinal dynamics. The terms W_e, U_e, and θ_e represent equilibrium values and depend on the selected operating point for which the linear model is generated. The X, Z, and M terms are the aerodynamic coefficients to be identified. The aerodynamic coefficients in the A'_{lon} matrix are referred to as stability derivatives, and the aerodynamic coefficients in the B'_{lon} matrix are referred to as control derivatives.

The longitudinal dynamics can be broken down into two dynamic modes: the phugoid mode and the short-period mode. The phugoid mode is typically slow, lightly damped, and dominates the response in states u and θ. The short-period mode is typically fast, moderately damped, and dominates the response in states w and q. Stability properties and pilot handling qualities of the aircraft depend primarily on the dynamics of the short-period mode. The short-period model takes the form of the system in Equation 1, but the state vector is $x = [w, q]$, and the matrices M'_{lon}, A'_{lon}, and B'_{lon} are given as

$$M_{lon} = \begin{bmatrix} m & 0 \\ 0 & I_y \end{bmatrix} \quad A'_{lon} = \begin{bmatrix} Z_w & Z_q + mU_e \\ M_w & M_q \end{bmatrix} \quad B'_{lon} = \begin{bmatrix} Z_{\delta_{elev}} \\ M_{\delta_{elev}} \end{bmatrix}$$

In addition to the longitudinal flight dynamics of the aircraft, the elevator actuator must be modeled. In general, actuators are modeled as low-pass filters, with bandwidth specifications provided by the hardware manufacturer. If such specifications are unavailable, the actuator dynamics are often neglected in the first iteration baseline model. Similarly, the time delay inherent to the system is also neglected in the baseline model. However, these effects are captured through the subsequent identification process.

2. Lateral/Directional Dynamics

The lateral/directional flight dynamics are described by the set of states $[v, p, r, \phi]$, which include body y-axis velocity v [m/s], roll rate p [rad/s], yaw rate r [rad/s], and bank angle ϕ [rad]. The control inputs to the lateral/directional model are aileron and rudder deflections, δ_{ail} [rad] and δ_{rud} [rad], respectively. The linearized equations of motion are given by the system in Equation 2.

$$M_{lat}\dot{x} = A'_{lat}x + B'_{lat}\begin{bmatrix} \delta_{ail} \\ \delta_{rud} \end{bmatrix} \tag{2}$$

where

$$M_{lat} = \begin{bmatrix} m & 0 & 0 & 0 \\ 0 & I_x & -I_{xz} & 0 \\ 0 & -I_{xz} & I_z & 0 \\ 0 & 0 & 0 & 1 \end{bmatrix} \quad A'_{lat} = \begin{bmatrix} Y_v & Y_p + mW_e & Y_r - mU_e & mgcos\theta_e \\ L_v & L_p & L_r & 0 \\ N_v & N_p & N_r & 0 \\ 0 & 1 & tan\theta_e & 0 \end{bmatrix} \quad B'_{lat} = \begin{bmatrix} Y_{\delta_{ail}} & Y_{\delta_{rud}} \\ L_{\delta_{ail}} & L_{\delta_{rud}} \\ N_{\delta_{ail}} & N_{\delta_{rud}} \\ 0 & 0 \end{bmatrix}$$

The terms Y, L, and N are the stability and control derivatives for the lateral/directional dynamics. Unlike the longitudinal dynamics, these dynamics cannot be broken down into decoupled modes. The lateral/directional dynamics are governed by a slow spiral mode, a fast lightly damped Dutch roll mode, and an even faster stable roll mode. Finally, the aileron and rudder actuators are modeled like the elevator actuator.

III. UAV Airframe and Wind Tunnel Testing

This section describes the Ultra Stick 25e flight test vehicle and the simple wind tunnel tests required to obtain a baseline model for its flight dynamics. The physical properties of the airframe and hardware capabilities are described in Subsection A. Simple wind tunnel tests and a baseline model of the flight dynamics are presented in Subsection B. Linear analysis is used to develop an understanding of the baseline aircraft dynamics before designing flight experiments and proceeding with system identification.

A. Airframe and Instrumentation

The Ultra Stick 25e has a conventional fixed-wing airframe with aileron, rudder, and elevator control surfaces. The aircraft is also equipped with flaps which are not used in this analysis. All control surfaces are actuated by electric servos with maximum deflection limits of 25 degrees in each direction. The propulsion system consists of an electric motor that drives a fixed-pitch propeller. Some important physical and geometric properties of the Ultra Stick 25e airframe are summarized in Table 1. A complete summary of the Ultra Stick 25e airframe can be found in Reference 9.

Table 1. Physical properties of the Ultra Stick 25e airframe.

Property	Symbol	Value	Units
Mass	m	1.943	kg
Wing Span	b	1.27	m
Wing Area	S	0.3097	m^2
Mean Aerodynamic Chord	c	0.25	m
Moment of Inertia	I_x	0.0894	$kg\ m^2$
Moment of Inertia	I_y	0.1444	$kg\ m^2$
Moment of Inertia	I_z	0.1620	$kg\ m^2$
Moment of Inertia	I_{xz}	0.0140	$kg\ m^2$

The aircraft is instrumented with several sensors that provide measurement of angular rates, accelerations, GPS position, and altitude. For simplicity, only the angular rate sensor is used for the system identification in this paper. The sensor is a rate gyroscope, and its noise band is around 4 deg/s. The aircraft is also equipped with an on-board flight computer upon which automatic control laws can be implemented. Sensor measurement data is recorded at 50 Hz. Takeoff and landing are performed manually by a pilot on the ground, while up and away flight can be handled by the flight computer. Flight is limited to line-of-sight range to avoid communication dropout and for safety. The aircraft is battery powered, allowing around 20 minutes of flying time on a single charge.

B. Wind Tunnel Tests and Analysis

To produce useful data for system identification, flight experiments are designed based on some a priori knowledge of the aircraft dynamics. For this purpose, a baseline model of the Ultra Stick 25e flight dynamics

is developed using simple wind tunnel tests on a scale model of the aircraft. The baseline model can be used to estimate the system gain and determine the relevant frequency range of the aircraft dynamics. Various empirical methods can be used to obtain such a model. The approach in this paper utilizes simple wind tunnel tests to obtain estimates for the stability and control derivatives.

The scale model is placed in a wind tunnel on a sting. Tunnel airspeed is held constant while aerodynamic forces and moments on the aircraft are measured by a sensor. The first two tests consist of sweeping angle-of-attack and sweeping angle of sideslip in discrete steps. The collected data is sufficient to estimate stability derivatives. Additionally, a third wind tunnel test is conducted to estimate the control derivatives by deflecting each surface independently and measuring the change in aerodynamic forces and moments.

Flight dynamics textbooks, such as Reference 8, contain formulas for calculating aircraft stability and control derivatives using wind tunnel force and moment data. This approach is used to estimate the derivatives for the longitudinal and lateral/directional dynamics of the Ultra Stick 25e. The terms in the model structure that depend specifically on the equilibrium flight condition can also be calculated from the wind tunnel data. Each derivative is non-dimensionalized by dynamic pressure and the geometry of the scale aircraft. The derivatives are then dimensionalized accordingly to the full-scale Ultra Stick 25e. This process is also described in Reference 8. The nominal flight condition for the full-scale aircraft is straight level flight at airspeed $V = 19\ m/s$. System identification flight experiments are performed at this operating point.

1. Longitudinal Dynamics

The longitudinal derivatives and equilibrium terms are calculated from wind tunnel data using the angle-of-attack sweep test. For example, the stability derivative Z_w is calculated using Equation 3.

$$Z_w = -\frac{\partial C_L}{\partial \alpha} - C_D \tag{3}$$

Using formulas such as Equation 3 from Reference 8, the stability and control derivatives in the longitudinal model can be approximated. The mass matrix is populated with data from Table 1. The resulting model is summarized by the matrices in Equation 4.

$$M_{lon} = \begin{bmatrix} 1.9430 & 0 & 0 & 0 \\ 0 & 1.9430 & 0 & 0 \\ 0 & 0 & 0.1444 & 0 \\ 0 & 0 & 0 & 1 \end{bmatrix}$$

$$A'_{lon} = \begin{bmatrix} -1.3819 & 1.4360 & -1.2068 & -19.0418 \\ -1.3612 & -15.1654 & 29.7756 & -0.6496 \\ 0.0226 & -1.2001 & -5.0843 & 0 \\ 0 & 0 & 1 & 0 \end{bmatrix} \quad B'_{lon} = \begin{bmatrix} 1.1994 \\ -7.1592 \\ -15.1901 \\ 0 \end{bmatrix} \tag{4}$$

For analysis of the dynamic modes of the aircraft, the longitudinal model is converted into conventional state-space form. This is accomplished by multiplying the system in Equation 1 by the left inverse of M_{lon}. The longitudinal model in conventional state-space form is shown in Equation 5, where the state matrix is represented by A_{lon} and the input matrix by B_{lon}.

$$\begin{aligned} M_{lon}^{-1} M_{lon} \dot{x} &= M_{lon}^{-1} A'_{lon} x + M_{lon}^{-1} B'_{lon} \delta_{elev} \\ \dot{x} &= A_{lon} x + B_{lon} \delta_{elev} \end{aligned} \tag{5}$$

Eigenvalue decomposition of the state matrix A_{lon} reveals the modes of the longitudinal dynamics. The phugoid mode has a natural frequency of 0.409 rad/s with a damping ratio of 0.91. The expected short-period mode does not exist in the baseline model. Instead, it is replaced by two stable real poles at 13.705 and 29.277 rad/s. This result is unconventional for fixed-wing aircraft, and is caused by the approximations made in the calculations of stability derivatives. However, this is not a major concern since the purpose of the baseline model is only to obtain general information about the aircraft dynamics to support flight experiment design. The estimated modes of the longitudinal dynamics are summarized in Table 2.

Table 2. Estimated modes of the longitudinal dynamics.

Mode	Natural Frequency [rad/s]	Damping Ratio
Phugoid	0.409	0.91
Short-Period Pole 1	13.705	-
Short-Period Pole 2	29.227	-

2. Lateral/Directional Dynamics

The lateral/directional derivatives are calculated from wind tunnel data acquired using the angle of sideslip sweep test. The populated matrices are shown in Equation 6.

$$M_{lat} = \begin{bmatrix} 1.943 & 0 & 0 & 0 \\ 0 & 0.0894 & -0.0140 & 0 \\ 0 & -0.0140 & 0.1620 & 0 \\ 0 & 0 & 0 & 1 \end{bmatrix}$$

$$A'_{lat} = \begin{bmatrix} -3.2856 & 1.2919 & -37.8665 & 19.0413 \\ -0.1918 & -1.2242 & 1.2220 & 0 \\ 0.1403 & 0.0037 & -1.0673 & 0 \\ 0 & 1 & 0.0341 & 0 \end{bmatrix} \quad B'_{lat} = \begin{bmatrix} 0 & 14.0113 \\ -6.1139 & 1.6334 \\ -1.0515 & -2.7712 \\ 0 & 0 \end{bmatrix} \tag{6}$$

The same method as used for the longitudinal analysis is applied to obtain the state and input matrices for the lateral/directional model, A_{lat} and B_{lat}, respectively. Eigenvalue decomposition of A_{lat} reveals the modes of the lateral/directional dynamics. The spiral mode has a pole at 0.047 rad/s, the Dutch roll mode has natural frequency of 6.027 rad/s with damping ratio 0.774, and the roll mode has a pole at 12.375 rad/s. This result agrees with typical dynamics of fixed-wing aircraft. The estimated modes of the longitudinal dynamics are summarized in Table 3.

Table 3. Estimated modes of the lateral/directional dynamics.

Mode	Natural Frequency [rad/s]	Damping Ratio
Spiral	0.047	-
Dutch Roll	6.027	0.774
Roll	12.375	-

The actuator dynamics and time delay in the system are considered unknown and neglected in the baseline model. The baseline model of the Ultra Stick 25e aircraft dynamics is used to design flight experiments needed for system identification. The next section describes input signal design for flight testing, as well as basic frequency domain system identification theory and its application to fixed-wing aircraft.

IV. Frequency Domain System Identification

Flight experiments are designed and carried out to obtain data for frequency domain system identification. Frequency domain system identification relies on the conversion of time domain flight data into the frequency domain. Frequency responses for the system are estimated for each input/output pair from the signals' spectral density functions. These frequency responses are then used to estimate stability and control derivatives. In this process, parametric transfer functions obtained directly from the model structure are fitted to the estimated frequency responses through nonlinear optimization. CIFER is used both to estimate the frequency responses and for the parametric identification.

This section is broken down into two parts. Subsection A describes the process of designing informative inputs for the flight experiments. Subsection B details the theoretical background to the frequency domain identification methods, and Subsection C presents the identified model.

A. Input Design for Flight Experiments

Two types of control inputs are considered for the flight test experiment. Frequency sweep input signals are utilized to excite the dynamics over a broad frequency range. These signals are comprised of sinusoids with continuously varying frequency over a selected interval. The data obtained from this test is used to extract frequency responses used for the model identification. The aircraft is also subjected to doublet inputs. These responses are utilized for time domain model verification.

The design of frequency sweep inputs must comply with several practical constraints. In a race track flight pattern, a maximum of 20 seconds of level flight can be achieved by the Ultra Stick 25e. However, due to trimming requirements after each turn, a 10 second experiment time window is about the longest possible for this experimental setup. As a result, frequencies below 0.1 Hz, or about 0.6 rad/s cannot be identified. Maximum frequency is given by the Nyquist sampling criteria. With a data sampling rate of 50 Hz, signals above 25 Hz cannot be recorded accurately. The fastest mode in the aircraft model is a short-period pole at around 30 rad/s, or about 5 Hz. Thus, a 7 Hz maximum frequency for the sweep input is sufficient to identify the relevant dynamics of the aircraft. Figure 2 shows the frequency response extracted from the baseline model for the pitch rate response to the elevator input. The applicable frequency range for frequency sweeps is shown to capture the majority of the relevant aircraft dynamics.

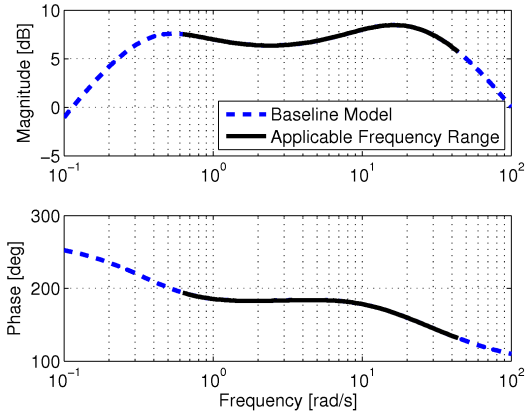

Figure 2. Applicable frequency range for system identification.

To achieve a sufficiently large signal-to-noise ratio (SNR), it is necessary that the output measurements exceed 8 deg/s. However, too large an input signal will take the aircraft too far from the nominal flight condition. Preliminary experiments showed that an output amplitude of 10 deg/s is sufficiently large to distinguish response from noise, yet maintain flight condition. Figure 3 shows an example time history for the elevator frequency sweep test. The elevator command signal is shown on top, and the pitch rate response is shown below. Note that the pitch rate response amplitude diminishes at higher frequencies, as expected from the bandwidth aircraft dynamics.

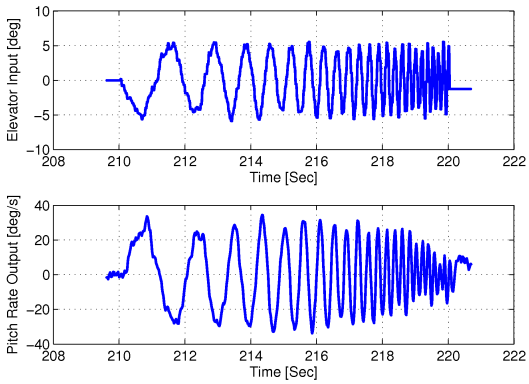

Figure 3. Sample elevator frequency sweep input signal and pitch rate response.

Repeated experiments are required to obtain sufficient high-quality flight data for system identification and model validation. Multiple frequency sweep experiments are conducted for each control surface to obtain a rich data set. From those, the best three are retained. Three doublet experiments are conducted for each control surface to ensure that at least one is free of major turbulence or other disturbances.

B. Theoretical Background

For applications of the type described in this paper, the frequency domain identification problem can be analyzed from a two-input, single-output system, shown in Figure 4.[10] The frequency domain relationship between each input and the output is determined first.

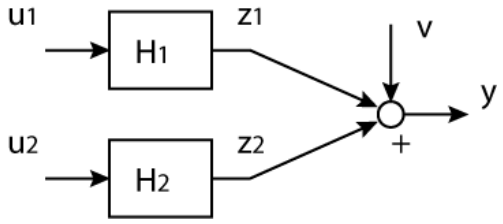

Figure 4. Diagram of a two-input, single-output system.

The signals u_1 and u_2 in Figure 4 represent the inputs to the system. The blocks H_1 and H_2 are transfer functions, and v is sensor measurement noise. It is assumed that v is white noise and uncorrelated with the input signals u_1 and u_2. Signal y is the measured system output. A multiple-output model, such as the lateral/directional model, can be constructed by superposing sets of these single-output relationships.

It is assumed that the inputs are statistically uncorrelated, which is accomplished experimentally by exciting control surface inputs independently. If the input signals are uncorrelated, the task to identify the transfer functions H_1 and H_2 is simple. Equation 7 describes the input-output relationship of the system in the frequency domain, where S represents a complex valued spectral density function.

$$S_{y,y}(\omega) = H_1(\omega)S_{u_1,u_1}(\omega) + H_2(\omega)S_{u_2,u_2}(\omega) \tag{7}$$

The transfer functions H_1 and H_2 are obtained from cross- and auto-spectral density functions S for the input and output signals. Equation 8 provides definitions for the transfer functions based on the spectral density functions.

$$H_1(\omega) = \frac{S_{y,u_1}(\omega)}{S_{u_1,u_1}(\omega)} \qquad H_2(\omega) = \frac{S_{y,u_2}(\omega)}{S_{u_2,u_2}(\omega)} \tag{8}$$

The spectral quantities in Equation 8 must be estimated. They are computed using CIFER, which implements an optimized windowing process to obtain the best bias/variance trade-off. Coherence functions γ^2 represent another important spectral quantity for frequency domain identification. They provide information about the linear correlation between inputs and outputs. A coherence value of one indicates that the entire output response is accounted for by the input via linear transfer function. A coherence value less than one implies the presence of non-ideal effects, such as nonlinear dynamics, unmeasured inputs, or measurement noise. High coherence, or above 0.7, is desired for accurate frequency domain system identification. Equation 9 defines coherence functions for the system in Figure 4 based on spectral density functions assuming uncorrelated inputs.

$$\gamma^2_{u_1,y}(\omega) = \frac{|S_{y,u_1}(\omega)|^2}{S_{u_1,u_1}(\omega)\ S_{y,y}(\omega)} \qquad \gamma^2_{u_2,y}(\omega) = \frac{|S_{y,u_2}(\omega)|^2}{S_{u_2,u_2}(\omega)\ S_{y,y}(\omega)} \tag{9}$$

Estimated frequency responses for the system dynamics are taken as the transfer functions H_1 and H_2. Coherence functions are used in the windowing process implemented to estimate the spectra. Understanding the experimental conditions under which the above assumptions are satisfied is fundamental to achieving accurate frequency response estimates. Once accurate frequency responses have been estimated, one of the greatest challenges of system identification is relating the dynamics captured by the frequency responses to corresponding parameters in a model structure. A nonlinear optimization is implemented to fit the estimated

frequency responses to parametric transfer functions associated with the model structure. The fitting process in CIFER is weighted based on coherence, emphasizing portions of the frequency response with high linear correlation.

The ability to identify parameters in a model structure depends on the number of free parameters in the equations of motion relative to the dynamics captured by the extracted frequency responses. It is possible to identify all derivatives in the model structure if every state is measured. However, this is typically not feasible with low-cost UAVs due to hardware and sensor limitations. As a result, some of the derivatives in the baseline model must be assumed to be fixed. It is crucial that the model structure being fitted is not over-parametrized relative to the dynamics contained in the extracted frequency responses.

The control derivatives, estimated from wind tunnel data, are assumed to be known in the case of the Ultra Stick 25e identification. This approach ensures that the model structure is not over-parametrized given output measurement limited to the angular rates. Additionally, the derivatives associated with the phugoid mode are assumed to be known. This assumption is required because the phugoid mode has a low natural frequency and is decoupled from the rest of the dynamics in the longitudinal axis, and thus impossible to identify given the ten second flight experiment time window.

C. Identification Results

Frequency domain system identification is applied separately to the longitudinal and lateral/directional dynamics. The simple structure of the short-period model is exploited to identify the actuator model and the system time delay. The actuator model and time delay are assumed to be the same for the entire aircraft.

1. Longitudinal Dynamics

The estimated frequency response from elevator input δ_{elev} to pitch rate output q is calculated using spectral density functions with CIFER. Nonlinear optimization is used to fit the model structure in Equation 1 to the estimated frequency response. The results are shown in Figure 5. The baseline model is shown in comparison to the identified model.

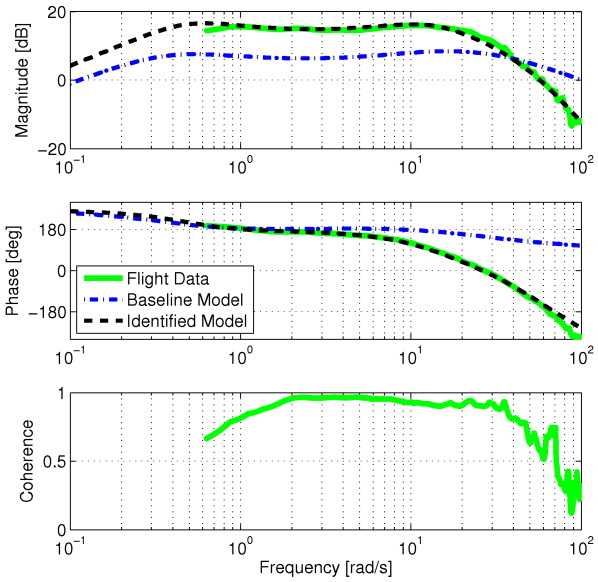

Figure 5. Longitudinal dynamics identification for elevator input to pitch rate.

The short-period is modeled as a two state system with full coupling in the state matrix. As a result, the short-period transfer function has relative degree one and exhibits a first-order roll-off. However, the estimated frequency response in Figure 5 exhibits a third-order roll-off, suggesting actuator dynamics with relative degree two. A second-order low-pass filter is identified for the actuator dynamics, resulting in a good fit of the magnitude curve. A Pade approximation is used for system time delay and allows a good fit of the phase curve. Table 4 summarizes the final identified model for the longitudinal aircraft dynamics.

Table 4. Identified longitudinal dynamics of the Ultra Stick 25e.

Mode	Frequency [rad/s]	Damping	Time Constant [sec]
Phugoid	0.497	0.724	12.652
Short-Period	13.390	0.736	0.452
Actuator	50.266	0.800	0.125
Time Delay			0.045

The identified A'_{lon} matrix is shown in Equation 10. Note that only stability derivatives corresponding to the short-period dynamics have been updated. The matrices M_{lon} and B'_{lon} are not changed as they are assumed to be known a priori.

$$A'_{lon} = \begin{bmatrix} -1.3819 & 1.4360 & -1.2068 & -19.0418 \\ -1.3612 & -17.3794 & 34.9752 & -0.6496 \\ 0.0226 & -0.6631 & -1.5563 & 0 \\ 0 & 0 & 1 & 0 \end{bmatrix} \tag{10}$$

The identified actuator model and system time delay are assumed to be the same for the entire aircraft and therefore are applied directly to the lateral/directional dynamics. This assumption is valid because all control surfaces are actuated by the same type of servo, and the measurement of all the outputs is obtained by the same sensor. As a result, the identification of the more complex lateral/directional dynamics is greatly simplified.

2. Lateral/Directional Dynamics

The four estimated frequency responses from aileron and rudder inputs δ_{ail} and δ_{rud} to pitch and yaw rate outputs p and r are calculated with the approach used for the longitudinal dynamics. The same nonlinear optimization is used to fit the model structure in Equation 2 to the estimated frequency responses simultaneously. Actuator models and system time delay identified for the longitudinal dynamics are applied to the lateral/directional dynamics. The results are shown for the aileron input to the angular rates in Figure 6, and for the rudder input to the angular rates in Figure 7. In all cases, the baseline model is shown in comparison to the final identified model.

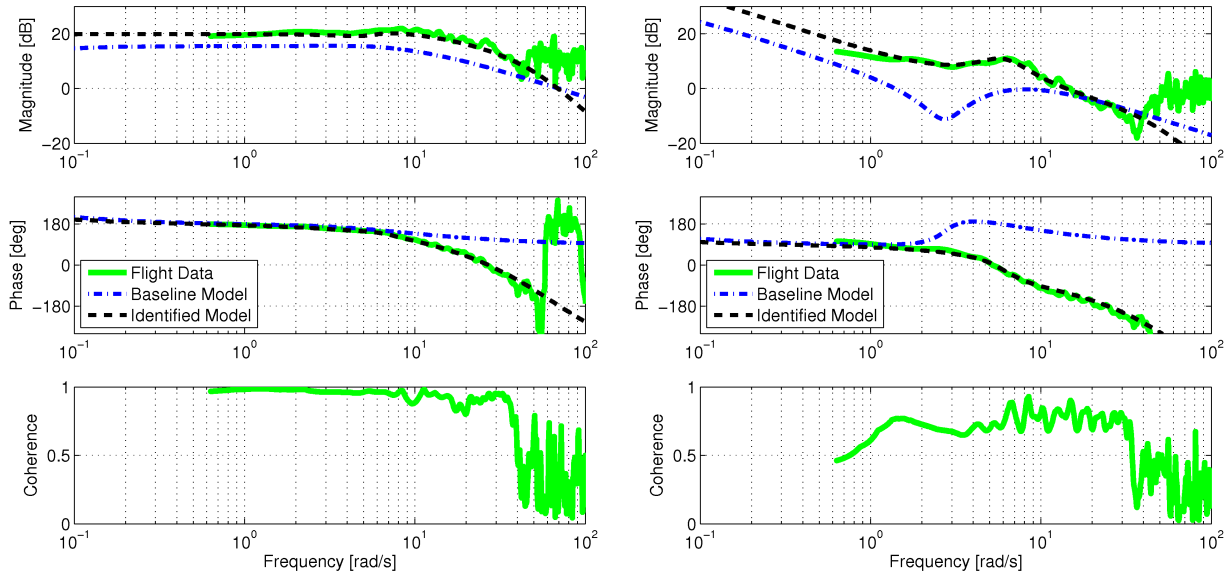

(a) Aileron input to roll rate.

(b) Aileron input to yaw rate.

Figure 6. Lateral/directional dynamics identification for aileron input.

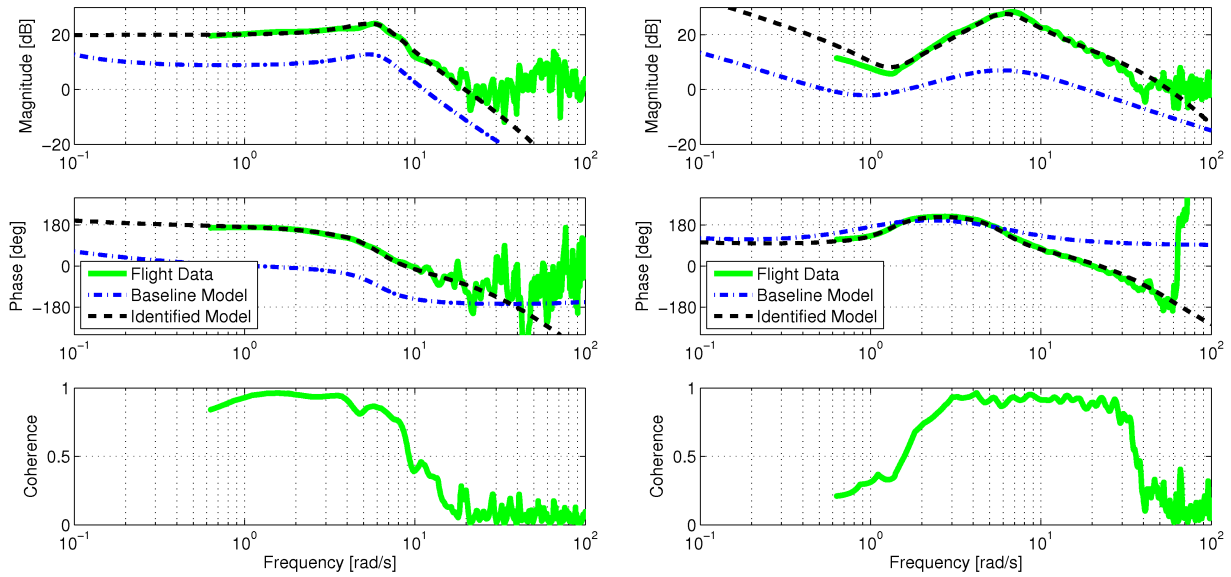

(a) Rudder input to roll rate.

(b) Rudder input to yaw rate.

Figure 7. Lateral/directional dynamics identification for rudder input.

Table 5 summarizes the final system identification results for the lateral/directional aircraft dynamics of the Ultra Stick 25e.

Table 5. Identified lateral/directional dynamics of the Ultra Stick 25e.

Mode	Frequency [rad/s]	Damping	Time Constant [sec]
Spiral	0.021		294.985
Dutch Roll	6.102	0.329	1.030
Roll	14.912		0.421

The identified A'_{lat} matrix is shown in Equation 11. Unlike for the longitudinal case, the entire set of lateral/directional stability derivatives are updated. The matrices M_{lat} and B'_{lat} are not changed as they are assumed to be known a priori.

$$A'_{lat} = \begin{bmatrix} -2.0031 & 1.2027 & -37.5089 & 19.0417 \\ -0.2654 & -1.3422 & 0.3398 & 0 \\ 0.2966 & 0.2934 & -0.4787 & 0 \\ 0 & 0 & 1 & 0 \end{bmatrix} \tag{11}$$

A full model of the Ultra Stick 25e flight dynamics is constructed using the results obtained from frequency domain system identification. The final step in the identification process is to validate the full model against flight data in the time domain.

V. Time Domain Model Validation

The accuracy of the identified aircraft model must be validated before it can be used for control design research. Time history flight data is used for the validation of the identified model. The full identified model of the Ultra Stick 25e dynamics is simulated using the input doublet signal from the flight experiment. The doublet input signal is designed as a sequence of maneuvers for each control surface. An elevator doublet is executed first, followed by a rudder doublet, and completed with an aileron doublet. The validation results are shown in Figure 8. The pitch rate response is shown on top, the roll rate response in the middle, and the yaw rate response on the bottom.

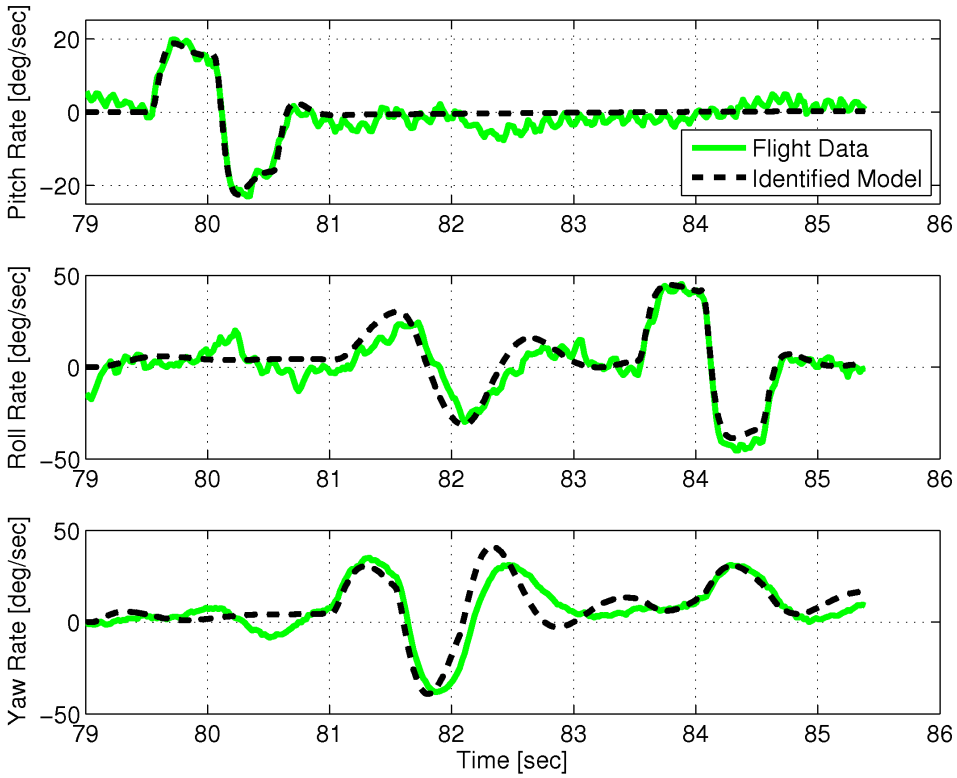

Figure 8. Time domain model validation of the Ultra Stick 25e identified dynamics.

The results in Figure 8 show that the identified model of the flight dynamics accurately predicts the true aircraft response. The pitch rate response confirms that the longitudinal dynamics are decoupled from the lateral/directional dynamics. Strong coupling is noted between the roll and yaw rate responses. The overall system gain is captured accurately. However, the true aircraft response in the rudder doublet exhibits a slight deviation from the response predicted by the identified model. This miss-match can be explained by a small offset in the natural frequency and damping of the Dutch roll mode.

System identification is ultimately an iterative process. The first iteration identified model represents a dramatic improvement in predicting the aircraft response compared to the original baseline model. The new model captures the primary dynamics of the aircraft and is suitable for use in control design and research applications. It can most likely be further refined by using the first iteration model to design more informative flight experiments, collect additional flight data, and repeat the analysis to improve accuracy.

VI. Conclusion

The goal of the work presented in this paper is focused on developing a rigorous and systematic procedure for frequency domain system identification applicable to small, low-cost, fixed-wing UAVs. This paper aims to serve as a guide for the steps necessary to determine an accurate model of the aircraft dynamics that is useful for flight control design and simulation.

The paper outlines all the steps in a rigorous and simple process for system identification. A model structure for the aircraft dynamics is derived along with the necessary assumptions required for simplification. Preliminary analysis using wind tunnel tests is used to construct a baseline model of the dynamics. The requirements to design informative flight experiment are presented, and frequency domain system identification theory is applied to the acquired data. Finally, the identified aircraft model is validated against time domain flight data. The results show that the identified aircraft model is able to accurately predict the primary dynamic modes of the aircraft. Therefore, it is ideally suited for flight control research applications.

Acknowledgments

The research summarized in this paper was started as a final project for a graduate level course in system identification in the Aerospace Engineering & Mechanics department at the University of Minnesota. The authors would like to specifically thank Ahmet Arda Ozdemir, Kamran Turkoglu, Paul Freeman, Michael Mott, and Navid Dadkhah for their contribution to this work.

References

[1]Ljung, L., *System Identification: Theory for the User*, Prentice Hall, 2nd ed., 1999.

[2]Klein, V. and Morelli, E. A., *Aircraft System Identification: Theory and Practice*, AIAA, Reston, VA.

[3]Mettler, B., Tischler, M., and Kanade, T., "System Identification of a Small-Scale Unmanned Rotorcraft for Flight Control Design," *Journal of the American Helicopter Society*, Vol. 47, No. 1, 2002.

[4]Theodore, C. and Tischler, M., "Rapid Frequency-Domain Modeling Methods for Unmanned Aerial Vehicle Flight Control Applications," *Journal of Aircraft*, Vol. 41, No. 4, 2004.

[5]Gremillion, G. and Humbert, J. S., "System Identification of a Quadrotor Micro Air Vehicle," *AIAA Atmospheric Flight Mechanics Conference and Exhibit, Toronto, Canada*, 2010.

[6]Murch, A., "UAV Research Group," http://www.uav.aem.umn.edu.

[7]Tischler, M. B. and Remple, R. K., *Aircraft and Rotorcraft System Identification*, AIAA, Reston, VA, 2006.

[8]Cook, M., *Flight Dynamics Principles*, Elsevier Ltd., 2nd ed., 2007.

[9]Murch, A. M., Paw, Y. C., Pandita, R., Li, Z., and Balas, G. J., "A Low Cost Small UAV Flight Research Facility," *CEAS Conference on Guidance, Navigation, and Control*, 2011.

[10]Bendal, J. S., *Engineering Applications of Correlation and Spectral Analysis*, John Wiley & Sons, New York, NY, 1993.